

Dalton Transactions

Accepted Manuscript



This is an *Accepted Manuscript*, which has been through the Royal Society of Chemistry peer review process and has been accepted for publication.

Accepted Manuscripts are published online shortly after acceptance, before technical editing, formatting and proof reading. Using this free service, authors can make their results available to the community, in citable form, before we publish the edited article. We will replace this *Accepted Manuscript* with the edited and formatted *Advance Article* as soon as it is available.

You can find more information about *Accepted Manuscripts* in the [Information for Authors](#).

Please note that technical editing may introduce minor changes to the text and/or graphics, which may alter content. The journal's standard [Terms & Conditions](#) and the [Ethical guidelines](#) still apply. In no event shall the Royal Society of Chemistry be held responsible for any errors or omissions in this *Accepted Manuscript* or any consequences arising from the use of any information it contains.

ARTICLE

A New Fluorescent Probe for Zn²⁺ with Red Emission and Its Application in Bioimaging

Cite this: DOI: 10.1039/x0xx00000x

Yiqun Tan, Min Liu, Junkuo Gao, Jiancan Yu, Yuanjing Cui, Yu Yang*, Guodong Qian*^aReceived 00th January 2012,
Accepted 00th January 2012

DOI: 10.1039/x0xx00000x

www.rsc.org/

A new fluorescent probe, (E)-3-(3-(4-([2,2':6',2''-terpyridin]-4'-yl)phenyl)acryloyl)-7-(diethylamino)-2H-chromen-2-one (ZC-F4) composed of coumarin as the fluorophore and terpyridine as the receptor is designed and synthesized. This probe exhibits good selectivity and sensitivity towards Zn²⁺ even on the ppb level with significant variation of emission wavelength (more than 100 nm shifts) after combined with Zn²⁺. One can observe the emission colour converted from green to red. Job's plot test suggests a 1:1 stoichiometry between ZC-F4 and Zn²⁺, and the theoretical calculation based on density functional theory has been carried out to get insight into the sensing mechanism. Furthermore, the imaging of Zn²⁺ in cells was also applied to test its feasibility in biology. This fluorescence probe would be a promising candidate for the applications in cell-imaging, environment protection, water treatment and safety inspection.

Introduction

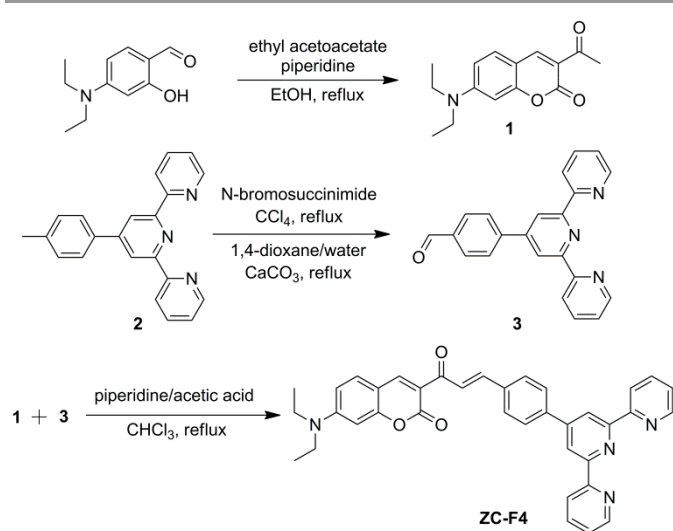
As the second most abundant transition metal ion in human body, zinc plays an important role in the gene transcription, regulation of metalloenzymes, neural signal transmission and apoptosis.¹⁻⁵ Its deficiency causes acrodermatitis enteropathica,⁶ while excess zinc may also cause serious neurological disorders such as Alzheimer's and Parkinson's diseases.⁷⁻⁹ It is found that the imbalance in zinc may cause several health problems including superficial skin diseases, prostate cancer, diabetes, and brain diseases.¹⁰⁻¹² Thus, extensive research efforts have been devoted on the quantitative measurement of trace Zn²⁺ in vivo.¹³⁻¹⁵ Because of the lack of spectroscopic signature of Zn²⁺, the method of fluorescence probe has become one of the best choices for detecting and tracking Zn²⁺ in cell-imaging and neuro-biological experiments.¹⁶

In recent years, a lot of fluorescent probes for detecting Zn²⁺ have been developed and most of them exhibit good performance in the cellular use.¹⁷⁻²⁷ However, many fluorescence sensors are still facing problems of selectivity, especially the interruption from Cd²⁺ which possesses very similar chemical properties with Zn²⁺ because of their location at the same group. Recently, Jiang et al. have reported an inspiring distinguishing method for Zn²⁺ and Cd²⁺ by introducing a carbonyl group.^{28, 29} Ng et al. designed two fluorescence sensors for differential detection of Zn²⁺ and Cd²⁺ based on BODIPY which can respond towards Zn²⁺ and Cd²⁺ respectively.³⁰ Lin et al. developed a single probe that displayed distinct responses to Zn²⁺ and Cd²⁺ depending on different

anions.³¹ Nevertheless, no reports about the application of these probes in cell-imaging were mentioned.

The development of novel fluorescence probes for metal ions with high sensitivity and selectivity has long been concerned by our group.³²⁻³⁵ We have developed a new fluorescence probe ZC-F1 based on intra-molecular transfer (ICT) effect for recognizing Zn²⁺ from Cd²⁺ with the detection limit under ppb level.³² But it cannot be used in bio-imaging for the following reasons: a) the poor solubility of ZC-F1 in aqueous solution restricts its application in vivo. b) The quantum yield of fluorophores bearing ICT effect usually reduces too much to apply in practice after the electron withdrawing group combined with metal ions, especially in solvents with high polarity, for the decrease of the energy gap between ground state and excited state.³⁶⁻³⁹ c) ZC-F1 emits green fluorescence after combined with Zn²⁺ with the emission located around 500 nm, while longer wavelength is in need for bio-imaging. To get over these obstacles, a new fluorescence probe highly sensitive and selective towards Zn²⁺ with better solubility and higher quantum yield is required.

Herein, we report a new fluorescence probe (E)-3-(3-(4-([2,2':6',2''-terpyridin]-4'-yl)phenyl)acryloyl)-7-(diethylamino)-2H-chromen-2-one (ZC-F4). This probe contains 7-diethylaminocoumarin, which is known as a water soluble fluorophore and terpyridine as the receptor for Zn²⁺.⁴⁰ To overcome the fluorescence decrease induced by metal ion binding, the carbonyl group is introduced as the electron withdrawing group, which conjugated with both coumarin and terpyridine. Then, Zn²⁺ will influence the electronegativity of



Scheme 1. Synthesis of ZC-F4

terpyridine instead of carbonyl directly. Thus, the influence of metal ions on the energy gap will be reduced largely and the fluorescence enhancement in aqueous solution can be expected, making it possible to detect and track Zn^{2+} in cell-imaging and cancer-biological experiments.

Experimental Section

Reagents and Apparatus

Solvents and reagents were obtained from commercial source and used as received without further purification.

^1H NMR spectra were recorded in CDCl_3 or $\text{DMSO}-d_6$ on a 500 MHz Bruker Avance DMX500 spectrometer with tetramethylsilane (TMS) as an internal standard. Elemental analysis was performed using a Thermo Finnigan Flash EA1112 microelemental analyzer. Differential scanning calorimetry (DSC) was performed on a Netzsch Instruments 200 F3 at a heating rate of 10 K/min under nitrogen atmosphere. Inductively coupled plasma spectroscopy (ICP) was performed on a Thermo XSENIES ICP-MS. Fluorescence emission spectra and excitation spectra were obtained on a Hitachi F4600 fluorescence spectrophotometer. UV-vis absorption spectra were obtained using a Perkin-Elmer Lambda spectrophotometer. All the theoretical calculations were performed based on density functional theory (DFT) at the B3LYP/6-31G(d) level.^{41, 42} The solvent effect on molecular geometries was included by means of the polarizable continuum model (PCM).^{43, 44} Based on the optimized geometry, all the molecular orbitals were calculated at the same level. All the calculations were performed in Gaussian09 software.⁴⁵ Fluorescence quantum yield is measured with integrating sphere on Edinburgh Instrument F900. Fluorescence images were obtained on confocal laser scanning microscopes (CLSM, fluoview FV1000, Olympus).

Synthesis

3-acetyl-7-(diethylamino)-2H-chromen-2-one (1): ethylacetoacetate (1.95 g, 15 mmol) and 4-diethylaminosalicylaldehyde (1.93 g, 10 mmol) was added into the solution of EtOH (20 mL), followed by the addition of piperidine (0.2 mL). The resulting mixture was refluxed for 6h and then cooled to room temperature. The yellow crystal was filtered and recrystallization was performed in EtOH to get pure product (1.55 g, 60%). ^1H NMR (500 MHz, CDCl_3): δ = 1.24(t, 6H, $J=7$ Hz, CH_2CH_3), 2.68(s, 3H, COCH_3), 3.45(m, 4H, $J=7$ Hz, CH_2CH_3), 6.47(d, 1H, $J=2.5$ Hz, ArH), 6.62(d, 1H, $J=9$ Hz, ArH), 7.39(d, 1H, $J=4$ Hz, ArH), 8.44(s, 1H, ArH). Anal. Calcd for $\text{C}_{15}\text{H}_{17}\text{NO}_3$: C, 69.48; N, 5.40; H, 6.61. Found: C, 69.83; N, 5.44; H, 6.64.

4-(p-methylphenyl)-2,2':6',2''-terpyridine (2): a solution of 4-methylbenzaldehyde (0.65 g, 5.4 mmol) and 2-acetylpyridine (1.3 g, 10.8 mmol) in methanol (120 mL) was added NaOH (0.22 g, 5.4 mmol) and NH_4OH 30 mL. The mixture was refluxed for 12h, and then cooled down to room temperature. The precipitate was filtered and washed by methanol and water to obtain white powder (1.05 g, 40%). ^1H NMR (500 MHz, CDCl_3): δ = 2.34(s, 3H, CH_3), 7.44(s, 2H, ArH), 7.67(d, 2H, $J=2$ Hz, ArH), 7.85(d, 2H, $J=8$ Hz, ArH), 7.97(s, 2H, ArH), 8.74(d, 2H, $J=7$ Hz, ArH), 8.78(t, 4H, $J=12$ Hz, ArH). Anal. Calcd for $\text{C}_{22}\text{H}_{17}\text{N}_3$: C, 81.71; N, 12.99; H, 5.30. Found: C, 81.59; N, 13.10; H, 5.31.

4-([2,2':6',2''-terpyridin]-4'-yl)benzaldehyde (3): **1** (1.0 g, 3.1 mmol) was added into the solution of CCl_4 (20 mL) and stirred for 15 min under the atmosphere of Ar_2 . Then, benzoyl peroxide (0.049 g, 0.2 mmol) and N-bromosuccinimide (1.23 g, 6.2 mmol) was added into the solution followed by reflux for 24h. The solution was cooled to room temperature and evaporated. The resulting yellow solid was then added into the solution of CaCO_3 (1.0 g, 10 mmol), 1,4-dioxane (40 mL) and water (10 mL) and refluxed for another 24h. The mixture was then cooled to room temperature, evaporated and purified by chromatography, using EtOAc and petroleum (1:2) as eluent, afforded pale solid **3** (0.50 g, 48%). ^1H NMR (500 MHz, CDCl_3): δ = 7.35(m, 2H, $J=5$ Hz, ArH), 7.87(m, 2H, ArH), 8.01(m, 4H, $J=8$ Hz, ArH), 8.66(d, 2H, $J=8$ Hz, ArH), 8.72(t, 4H, ArH), 10.8(s, 1H, CHO). Anal. Calcd for $\text{C}_{22}\text{H}_{15}\text{N}_3\text{O}$: C, 78.32; N, 12.46; H, 4.48. Found: C, 78.39; N, 12.50; H, 4.41.

(E)-3-(3-(4-([2,2':6',2''-terpyridin]-4'-yl)phenyl)acryloyl)-7-(diethylamino)-2H-chromen-2-one (ZC-F4): **1** (1.55 g, 6 mmol) and **3** (1.34 g, 4 mmol) was resolved in CHCl_3 (20 mL) followed by the addition of piperidine (0.1 mL) and acetate acid (0.2 mL) and refluxed for 24h. After cooling to room temperature, the resulting mixture was then extracted three times. The organic phase was combined, dried with MgSO_4 . The solvent was removed under reduced pressure and the remaining black powder was purified by chromatography, using CH_2Cl_2 and EtOAc (20:1) to yield orange solid **ZC-F4** (1.41 g, 61%). ^1H NMR (500 MHz, CDCl_3): δ = 1.25(t, 6H, $J=5$ Hz, CH_2CH_3), 3.47(m, 4H, $J=7.5$ Hz, CH_2CH_3), 6.50(s, 1H, ArH), 6.63(d, 1H, $J=9$ Hz, ArH), 7.36(m, 2H, ArH), 7.43(d, 1H, $J=9$ Hz, ArH), 7.82(d, 2H, $J=8$ Hz, $\text{CH}=\text{CH}$), 7.88(m, 3H, ArH), 7.94(d, 2H, $J=8$ Hz, ArH), 8.23(d, 1H, $J=16$ Hz, ArH), 8.57(s,

1H, ArH), 8.67(d, 2H, J=8 Hz, ArH), 8.74(m, 4H, ArH). Anal. Calcd for $C_{37}H_{30}N_4O_3$: C, 76.80; N, 9.68; H, 5.23. Found: C, 76.69; N, 9.80; H, 5.31.

Zn(ZC-F4)(NO₃)₂(H₂O)₂ (ZC-F4-Zn): ZC-F4 (0.058 g, 0.1 mmol) was resolved in CHCl₃ (3mL) followed by the addition of Zn(NO₃)₂ (0.057 g, 0.3 mmol) in 5 mL methanol. Upon mixing, a deep red suspension formed immediately. The resulting mixture was stirred for another 15 min to ensure a complete reaction. The red solid was obtained by filtration, and then washed by ethanol (5 mL×3). ¹H NMR (500 MHz, DMSO-D₆): δ = 1.17 (t, 6H, J=7 Hz, CH₂CH₃), 3.53 (m, 4H, CH₂CH₃), 6.64 (s, 1H, ArH), 6.85 (d, 1H, J=8.5 Hz, ArH), 7.52 (t, 1H, J=6 Hz, ArH), 7.74 (d, 1H, J=9 Hz, ArH), 7.85 (m, 1H, ArH), 7.99 (m, 2H, ArH), 8.04 (d, 1H, J=8Hz, ArH), 8.12 (d, 2H, J=8Hz, CH=CH), 8.31 (t, 2H, J=7.5Hz, ArH), 8.54 (d, 2H, J=8 Hz, ArH), 8.67 (s, 1H, ArH), 8.91 (d, 1H, J=4 Hz), 9.10 (d, 1H, J=8Hz, ArH), 9.18 (d, 2H, J=8.5 Hz, ArH), 9.46 (s, 1H, ArH). Anal. Cal. for $C_{37}H_{34}N_6O_{11}Zn$: C, 55.27; N, 10.45; H, 4.26. Found: C, 55.00; N, 10.37; H, 4.04.

To certify the ratio between ZC-F4 and Zn²⁺ in ZC-F4-Zn, ICP experiment was conducted by resolving 5 mg complex into 20 mL aqueous solution (DMSO:H₂O=1:99) followed by addition of 100 μL hydrochloric acid. The concentration of Zn²⁺ found in the solution is 20.5 mg/L, agree with that calculated (20.3 mg/L).

Cell Culture

HeLa human cervical carcinoma cells were cultured in Dulbecco's Modified Eagle's Medium (DMEM, Neuronbc) supplemented with 10 % fetal bovine serum (FBS, sijiqing) penicillin (100 units/ml, Boster), and streptomycin (100 μg/mL, Boster). Two days before imaging, the cells were passed and plated on glass-bottomed dishes. For labeling, the growth medium was removed and replaced with DMEM without FBS. The cells were treated and incubated with 10 μL of 1 mM ZC-F4 in DMSO stock solution (10 μM ZC-F4) at 37 °C under 5 % CO₂ for 15 min, and provided with 5μL of fresh media that contained either 1 mM or 0 mM ZnCl₂. Then, the cells were incubated for another 15 min at the conditions mentioned above. Prior to imaging, cells were rinsed three times with phosphate buffered saline (PBS).

Results and Discussion

Design and Synthesis of ZC-F4

In the newly designed fluorescence probe ZC-F4, 7-diethylaminocoumarin is selected as the fluorophore to improve its solubility in water, and 2,2',6',2''-terpyridine is selected as the receptor for Zn²⁺ for its good performance in previous work. In addition, amino group possess strong electron-donating ability, which may strengthen ICT effect and large Stokes' shifts, leading to red emission.⁴⁶⁻⁴⁹ However, unlike ZC-F1, the fluorophore and the receptor are not conjugated directly, but linked via carbonyl group. So ICT is established between carbonyl group and the diethylamino part,⁵⁰⁻⁵² while terpyridine

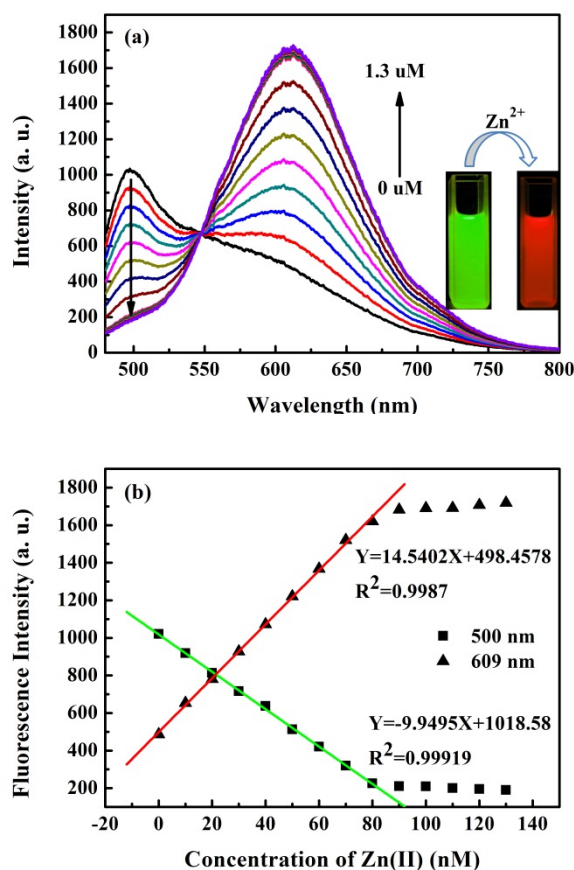


Figure 1. (a) Fluorescence emission spectra of ZC-F4 (100 nM) excited at 468 nm upon titration of Zn²⁺ at the concentration of 0, 10, 20, 30, 40, 50, 60, 70, 80, 90, 100, 110, 120, 130 nM. Insets: luminescent photos of ZC-F4 before and after the addition of Zn²⁺ under the excitation of a 315 nm UV lamp. (b) Fluorescence intensities observed at 500 nm and 609 nm as a function of the [Zn²⁺].

impact on the carbonyl group with its weak electron-withdrawing ability. As a result, the zinc ions will influence on the electronegativity of the electron acceptor indirectly after combined with terpyridine, which suggests weak influence on ICT energy level. Thus, an improved fluorescence emission of ZC-F4 in aqueous solution can be expected.

As shown in Scheme 1, the compound ZC-F4 can be synthesized in several steps from commercially available chemicals in high yield. Details for synthesis are described in the experiment section.

Optical Response of Probe ZC-F4

To test its feasibility for Zn²⁺ detection, the fluorescence spectra and the response of ZC-F4 after titrated with Zn²⁺ are first studied in aqueous solution (water : DMSO = 99 : 1). As shown in Figure 1(a), a broadband emission spectrum with peaks located at 500 nm can be observed when excited at 468 nm. While this emission band gradually disappeared with the titration of Zn²⁺ and a new emission band located at 609 nm

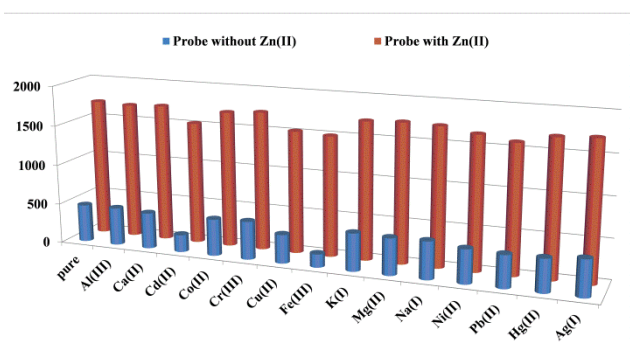


Figure 2. Fluorescence intensities of ZC-F4 (100 nM in water:DMSO=99:1) towards Zn^{2+} and various interferences (40 equiv. for K^+ , Ca^{2+} , Na^+ and Al^{3+} and 20 equiv. for others) at 609 nm upon excitation at 468 nm.

owing to the combination of ZC-F4 and Zn^{2+} can be observed. Significant enhancement of fluorescence intensity can be observed even when $[\text{Zn}^{2+}]$ is as low as 10 nM, which equals to 0.65 ppb, indicating that ZC-F4 is highly sensitive for Zn^{2+} even at ppb level. It is worth to be noted that the fluorescence intensities of ZC-F4 at both 500 nm and 609 nm have well fitted linearship with the concentration of Zn^{2+} (Figure 1(b)), suggesting its usage for quantitative detection of Zn^{2+} . The absorption response of ZC-F4 towards Zn^{2+} show that the absorption maximum shift from 450 nm to 468 nm with a Isosbestic point located at 456 nm, indicating the formation of the complex of ZC-F4 with Zn^{2+} (Figure S1). Job's plot analysis suggests a 1:1 stoichiometry (Figure S2).

To verify the application of ZC-F4 in complicated environment, metal ions with biological and environmental interests such as Ni^{2+} , Cd^{2+} , Cr^{3+} , Fe^{3+} , Na^+ , Ca^{2+} , Pb^{2+} , Al^{3+} , Co^{2+} , Cu^{2+} , Mg^{2+} , K^+ , Hg^{2+} and Ag^+ have been introduced as the interferences to investigate their impact on the selectivity of ZC-F4 towards Zn^{2+} . As we can see in Figure 2, main group metal ions and some transition metal ions, including K^+ , Ca^{2+} , Na^+ , Mg^{2+} , Al^{3+} , Co^{2+} , Cr^{3+} , Ni^{2+} and Pb^{2+} exhibit almost no

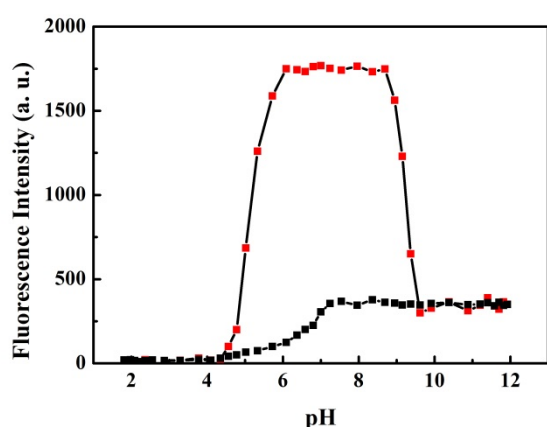


Figure 3. Fluorescence intensities of ZC-F4 (black) and ZC-F4-Zn (red, $[\text{ZC-F4}] = 100 \text{ nM}$, $[\text{Zn}^{2+}] = 100 \text{ nM}$) at 609 nm at various pH conditions in aqueous solution (water:DMSO=99:1). $\lambda_{\text{ex}} = 468 \text{ nm}$

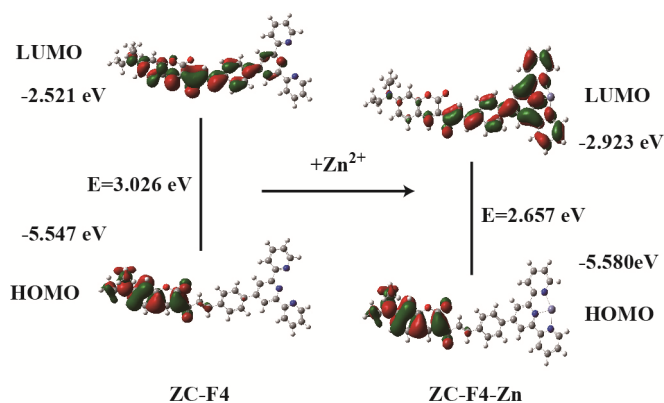


Figure 4. HOMO-LUMO energy levels and the interfacial plots of the molecular orbitals for ZC-F4 and its complex form with Zn^{2+} (ZC-F4-Zn)

influence on the fluorescence response of ZC-F4 before and after the addition of Zn^{2+} , while Cu^{2+} and Fe^{3+} exert slightly quenching effect resulted from their strong absorption of light. However, compared with the strong fluorescence enhancement caused by Zn^{2+} , their disturbances are quite minor. Although fluorescence variation can be observed when Cd^{2+} was added into ZC-F1 in our previous work, ZC-F4 shows no fluorescence responses towards Cd^{2+} except minor quenching effect. This might be due to the weaker Lewis acidity of Cd^{2+} compared with Zn^{2+} , while different molecular structure between ZC-F1 and ZC-F4 may also help to recognize Zn^{2+} from Cd^{2+} . In addition, Hg lies in the same group as Zn and Cd, but Hg^{2+} and its common interference Ag^+ exhibit no disturbance.

pH effect

To verify its potential usage in biology, pH effect on the fluorescence response of the probe is investigated by plotting the fluorescence intensity of ZC-F4 with Zn^{2+} vs pH values. As shown in Figure 3, the emission intensities of the probe increased dramatically with pH increase from 4.5 to 6 which can be ascribed to the competition between the proton and zinc ions. Meanwhile, stable fluorescence towards Zn^{2+} can be observed in the pH range 6-9, indicating that the probe is suitable for biology use. The fluorescence of ZC-F4-Zn quenched under alkaline conditions with $\text{pH} > 9$, which can be well explained by the formation of $\text{Zn}(\text{OH})^-$ or $\text{Zn}(\text{OH})_2$ and thus reducing the concentration of Zn^{2+} .

Theoretical Calculations

To get insight into the probing mechanism, computations on the probe before and after combination with Zn^{2+} is performed based on density functional theory (DFT).

As shown in Figure 4, electrons mainly localized on the coumarin part at ground state and transfer to the carbonyl group and the atoms around when excited, indicating a moderate ICT effect in the molecule. It is worth to be noted that the two end-capped pyridine rings are not coplanar to the other part of the molecule, while they didn't take part in the electron rearrangement, suggesting its weak influence on the charge

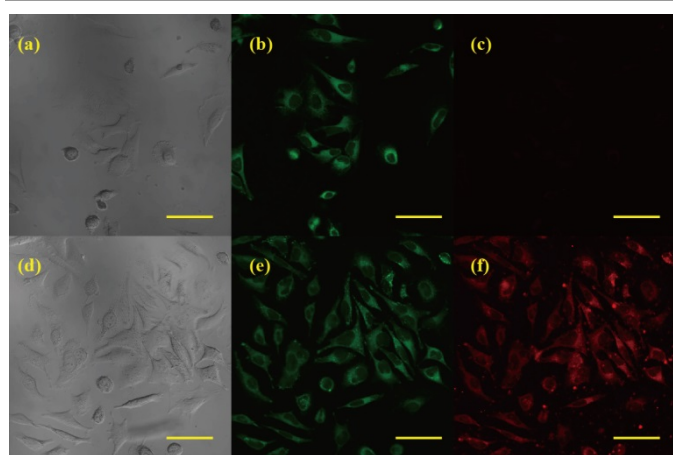


Figure 5. Images of HeLa cells incubated with ZC-F4 (10 μM) and ZnCl_2 at the concentration of 0 μM (a-c) and 5 μM (d-f) for 30 min. Panels (a) and (d) show differential interference contrast (DIC) images, while Panels (b), (c), (e) and (f) show the corresponding confocal fluorescence images collected at 450-530 nm (b and e) and 550-650 nm (c and f). The wavelength for excitation is 405 nm. The scale bar is 50 μm .

transfer effect. However, when Zn^{2+} coordinated with the probe, the electrons are still located on the coumarin part at the ground state, but rearranged to the part from carbonyl to the terpyridine group when excited, showing that terpyridine also participate in the ICT effect. This electron rearrangement was enhanced owing to the strong electronegativity of terpyridine after combined with Zn^{2+} , resulting in large Stokes' shift and red emission. Meanwhile, the pyridine rings have the same orientation within the conjugated plane, which may also enhance the ICT effect and fluorescence quantum yield by improving the conjugation. Thus, the enhancement of fluorescence and Stokes' shift can be realized.

Cell imaging

Since the probe has exhibited excellent sensing properties for Zn^{2+} in vitro, the assessment whether ZC-F4 can detect Zn^{2+} in live cells is possible by labelling HeLa cells with the probe. As controls, the cells were incubated with 10 μM ZC-F4 for 30 min in DMEM medium at 37 $^\circ\text{C}$, which showed strong intracellular fluorescence in the window of 480-550 nm, while no fluorescence displayed in the detection range of 570-700 nm. Then, these cells were incubated with DMEM containing ZnCl_2 (5 μM) for another 15 min at 37 $^\circ\text{C}$. After incubation, these cells were washed with PBS three times and dramatically enhanced fluorescence emission in the range of 570-700 nm can be observed (excitation at 468 nm) (Figure 5). The results of the bright-field measurements (Fig. 5a and 5d) suggested that the cells were viable throughout the imaging experiments upon treatment with ZC-F4 and Zn^{2+} , respectively. As depicted, these dramatic changes suggested that ZC-F4 was membrane permeable and could response to the presence of Zn^{2+} in live cells. It can be supplied as a useful probe for studying the distribution and physiological activity of Zn^{2+} in live cells.

Conclusion

In summary, a new fluorescence probe (ZC-F4) towards Zn^{2+} was designed and synthesized and its response was studied. This probe could recognize Zn^{2+} with signals in two channels. Meanwhile, ZC-F4 was highly sensitive to Zn^{2+} on the ppb level with little disturbances from other competing metal ions, confirming its good selectivity. Furthermore, the cell imaging experiments showed that ZC-F4 was cell permeable for biology use and it can be supplied as a useful probe for studying the distribution and physiological activity of Zn^{2+} in live cells.

Acknowledgements

The authors gratefully acknowledge the financial support for this work from the National Natural Science Foundation of China (Nos. 51010002, 51272231, 51229201 and 51372221), Natural Science Foundation of Zhejiang Province (No. LY12E02004), and the Fundamental Research Funds for the Central Universities.

Notes and references

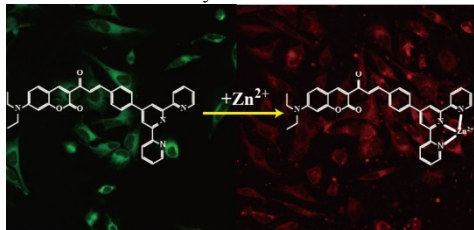
^a State Key Laboratory of Silicon Materials, Cyrus Tang Center for Sensor Materials and Applications, Department of Materials Science & Engineering, Zhejiang University, Hangzhou, China. E-mail: gdqian@zju.edu.cn (G. Qian). yuyang@zju.edu.cn (Y. Yang) Electronic Supplementary Information (ESI) available: Supplementary spectra data. See DOI: 10.1039/b000000x/

1. J. M. Berg and Y. Shi, *Science*, 1996, **271**, 1081-1085.
2. C. J. Frederickson and A. I. Bush, *BioMetals*, 2001, **14**, 353-366.
3. B. L. Vallee and K. H. Falchuk, *Phys. Rev.*, 1993, **73**, 79-118.
4. A. Voegelin, S. Pfister, A. C. Scheinost, M. A. Marcus and R. Kretzschmar, *Environ. Sci. Technol.*, 2005, **39**, 6616-6623.
5. X. Xie and T. G. Smart, *Nature*, 1991, **349**, 521-524.
6. S. Kury, B. Dreno, S. Bezieau, S. Giraudet, M. Kharfi, R. Kamoun and J.-P. Moisan, *Nat Genet*, 2002, **31**, 239-240.
7. A. I. Bush, W. H. Pettingell, M. D. Paradis and R. E. Tanzi, *J. Biol. Chem.*, 1994, **269**, 12152-12158.
8. M. P. Cuajungco and G. J. Lees, *Neurobiology of Disease*, 1997, **4**, 137-169.
9. J.-Y. Koh, S. W. Suh, B. J. Gwag, Y. Y. He, C. Y. Hsu and D. W. Choi, *Science*, 1996, **272**, 1013-1016.
10. E. Kimura, S. Aoki, E. Kikuta and T. Koike, *Proc. Natl. Acad. Sci. U. S. A.*, 2003, **100**, 3731-3736.
11. A. Truong-Tran, J. Carter, R. Ruffin and P. Zalewski, *Biometals*, 2001, **14**, 315-330.
12. P. D. Zalewski, I. J. Forbes, R. F. Seemark, R. Borlinghaus, W. H. Betts, S. F. Lincoln and A. D. Ward, *Chemistry & Biology*, 1994, **1**, 153-161.
13. A. N. Anthemidis and C.-P. P. Karapatouchas, *Microchimica Acta*, 2008, **160**, 455-460.
14. A. C. Davis, C. P. Calloway Jr and B. T. Jones, *Talanta*, 2007, **71**, 1144-1149.
15. G. Kaya and M. Yaman, *Talanta*, 2008, **75**, 1127-1133.
16. Z. Xu, J. Yoon and D. R. Spring, *Chem. Soc. Rev.*, 2010, **39**, 1996-2006.

17. N. Y. Baek, C. H. Heo, C. S. Lim, G. Masanta, B. R. Cho and H. M. Kim, *Chem. Commun.*, 2012, **48**, 4546-4548.
18. X. Chen, J. Shi, Y. Li, F. Wang, X. Wu, Q. Guo and L. Liu, *Org. Lett.*, 2009, **11**, 4426-4429.
19. T. Cheng, T. Wang, W. Zhu, X. Chen, Y. Yang, Y. Xu and X. Qian, *Org. Lett.*, 2011, **13**, 3656-3659.
20. H. M. Kim and B. R. Cho, *Accounts Chem. Res.*, 2009, **42**, 863-872.
21. G. Masanta, C. S. Lim, H. J. Kim, J. H. Han, H. M. Kim and B. R. Cho, *J. Am. Chem. Soc.*, 2011, **133**, 5698-5700.
22. X. Meng, S. Wang, Y. Li, M. Zhu and Q. Guo, *Chem. Commun.*, 2012, **48**, 4196-4198.
23. K. Sreenath, J. R. Allen, M. W. Davidson and L. Zhu, *Chem. Commun.*, 2011, **47**, 11730-11732.
24. H. Tian, B. Li, J. Zhu, H. Wang, Y. Li, J. Xu, J. Wang, W. Wang, Z. Sun, W. Liu, X. Huang, X. Yan, Q. Wang, X. Yao and Y. Tang, *Dalton Trans.*, 2012, **41**, 2060-2065.
25. Y. Pourghaz, P. Dongare, D. W. Thompson and Y. Zhao, *Chem. Commun.*, 2011, **47**, 11014-11016.
26. Z. Xu, K.-H. Baek, H. N. Kim, J. Cui, X. Qian, D. R. Spring, I. Shin and J. Yoon, *J. Am. Chem. Soc.*, 2009, **132**, 601-610.
27. S. Yin, J. Zhang, H. Feng, Z. Zhao, L. Xu, H. Qiu and B. Tang, *Dyes Pigment.*, 2012, **95**, 174-179.
28. L. Xue, C. Liu and H. Jiang, *Org. Lett.*, 2009, **11**, 1655-1658.
29. L. Xue, Q. Liu and H. Jiang, *Org. Lett.*, 2009, **11**, 3454-3457.
30. H. He and D. K. Ng, *Chem.-Asian J.*, 2013, **8**, 1441-1446.
31. J. Wang, W. Lin and W. Li, *Chem.—Eur. J.*, 2012, **18**, 13629-13632.
32. Y. Tan, J. Gao, J. Yu, Z. Wang, Y. Cui, Y. Yang and G. Qian, *Dalton Trans.*, 2013, **42**, 11465-11470.
33. Y. Tan, J. Yu, J. Gao, Y. Cui, Z. Wang, Y. Yang and G. Qian, *RSC Adv.*, 2013, **3**, 4872-4875.
34. Y. Tan, J. Yu, J. Gao, Y. Cui, Y. Yang and G. Qian, *Dyes Pigment.*, 2013, **99**, 966-971.
35. Y. Tan, J. Yu, Y. Cui, Y. Yang, Z. Wang, X. Hao and G. Qian, *Analyst*, 2011, **136**, 5283-5286.
36. A. Marini, A. Muñoz-Losa, A. Biancardi and B. Mennucci, *J. Phys. Chem. B*, 2010, **114**, 17128-17135.
37. R. S. Mulliken, *J. Phys. Chem.*, 1952, **56**, 801-822.
38. R. S. Mulliken, *J. Am. Chem. Soc.*, 1952, **74**, 811-824.
39. J. Wu, W. Liu, J. Ge, H. Zhang and P. Wang, *Chem. Soc. Rev.*, 2011, **40**, 3483-3495.
40. Z. Jiang, H. Lv, J. Zhu and B. Zhao, *Synthetic Metals*, 2012, **162**, 2112-2116.
41. A. D. Becke, *J. Chem. Phys.*, 1993, **98**, 5648.
42. W. J. Hehre, *J. Chem. Phys.*, 1972, **56**, 2257.
43. M. Cossi, N. Rega, G. Scalmani and V. Barone, *J. Comput. Chem.*, 2003, **24**, 669-681.
44. J. Tomasi, B. Mennucci and R. Cammi, *Chem. Rev.*, 2005, **105**, 2999-3094.
45. R. A. Gaussian 09, Frisch, M. J.; Trucks, G. W.; Schlegel, H. B.; Scuseria, G. E.; Robb, M. A.; Cheeseman, J. R.; Scalmani, G.; Barone, V.; Mennucci, B.; Petersson, G. A.; Nakatsuji, H.; Caricato, M.; Li, X.; Hratchian, H. P.; Izmaylov, A. F.; Bloino, J.; Zheng, G.; Sonnenberg, J. L.; Hada, M.; Ehara, M.; Toyota, K.; Fukuda, R.; Hasegawa, J.; Ishida, M.; Nakajima, T.; Honda, Y.; Kitao, O.; Nakai, H.; Vreven, T.; Montgomery, Jr., J. A.; Peralta, J. E.; Ogliaro, F.; Bearpark, M.; Heyd, J. J.; Brothers, E.; Kudin, K. N.; Staroverov, V. N.; Kobayashi, R.; Normand, J.; Raghavachari, K.; Rendell, A.; Burant, J. C.; Iyengar, S. S.; Tomasi, J.; Cossi, M.; Rega, N.; Millam, J. M.; Klene, M.; Knox, J. E.; Cross, J. B.; Bakken, V.; Adamo, C.; Jaramillo, J.; Gomperts, R.; Stratmann, R. E.; Yazyev, O.; Austin, A. J.; Cammi, R.; Pomelli, C.; Ochterski, J. W.; Martin, R. L.; Morokuma, K.; Zakrzewski, V. G.; Voth, G. A.; Salvador, P.; Dannenberg, J. J.; Dapprich, S.; Daniels, A. D.; Farkas, Ö.; Foresman, J. B.; Ortiz, J. V.; Cioslowski, J.; Fox, D. J. Gaussian, Inc., Wallingford CT, 2009.
46. J. Delcamp, Y. Shi, J. Yum, T. Sajoto, E. Dell'orto, S. Barlow, M. Nazeeruddin, S. Marder and M. Gratzel, *Chem.—Eur. J.*, 2013, **19**, 1819-1827.
47. N. Karton-Lifshin, L. Albertazzi, M. Bendikov, P. S. Baran and D. Shabat, *J. Am. Chem. Soc.*, 2012, **134**, 20412-20420.
48. Y.-Y. Wu, Y. Chen, G.-Z. Gou, W.-H. Mu, X.-J. Lv, M.-L. Du and W.-F. Fu, *Org. Lett.*, 2012, **14**, 5226-5229.
49. Y. Tan, Q. Zhang, J. Yu, X. Zhao, Y. Tian, Y. Cui, X. Hao, Y. Yang and G. Qian, *Dyes Pigment.*, 2013, **97**, 58-64.
50. H. M. Kim, M. S. Seo, M. J. An, J. H. Hong, Y. S. Tian, J. H. Choi, O. Kwon, K. J. Lee and B. R. Cho, *Angew. Chem.-Int. Edit.*, 2008, **47**, 5167-5170.
51. D. M. Nguyen, A. Frazer, L. Rodriguez and K. D. Belfield, *Chem. Mat.*, 2010, **22**, 3472-3481.
52. B. Zhu, C. Gao, Y. Zhao, C. Liu, Y. Li, Q. Wei, Z. Ma, B. Du and X. Zhang, *Chem. Commun.*, 2011, **47**, 8656-8658.

ARTICLE

Table of contents entry:



Selectively probing Zn²⁺ in vivo! A new fluorescent probe highly sensitive and selective for Zn²⁺ based on ICT effect was designed. This probe exhibited potential application in biological usage.